Applied Catalysis B: Environmental 164 (2015) 360–370

Contents lists available at ScienceDirect

Applied Catalysis B: Environmental

journal homepage: www.elsevier.com/locate/apcatb

Interaction of H_2S with ZrO_2 and its influence on reactivity of surface oxygen

E.I. Kauppi[a,*], J.M. Kanervo[a], J. Lehtonen[a], L. Lefferts[a,b]

[a] Aalto University, School of Chemical Technology, Department of Biotechnology and Chemical Technology, Research Group Industrial Chemistry, P.O. Box 16100, 00076 Aalto, Finland
[b] University of Twente, Faculty of Science & Technology and MESA+ Institute for Nanotechnology, P.O. Box 217, 7500 AE Enschede, The Netherlands

ARTICLE INFO

Article history:
Received 1 July 2014
Received in revised form
15 September 2014
Accepted 20 September 2014
Available online 8 October 2014

Keywords:
ZrO_2
Biomass gasification gas clean-up
H_2S adsorption
TPD
H_2-TPR
CO-TPR

ABSTRACT

ZrO_2 catalysts can be efficiently applied to convert tars into less harmful compounds in biomass gasification gas clean-up, also in the presence of H_2S. In fact, H_2S has even been observed to enhance naphthalene (a model compound for tar) oxidation activity on ZrO_2. Sulfur binding and its effect on the reactivity of surface oxygen species, including OH groups as well surface lattice oxygen, on ZrO_2 was studied using temperature-programmed methods. At 30 °C approx. half of the adsorbed H_2S was physisorbed and the other part dissociated titrating terminal OH groups. This dissociated H_2S was strongly adsorbed. Moreover, it was found that after treatment with H_2S until 400 °C half of the adsorbed species were irreversibly adsorbed. H_2S adsorbed inducing desorption of water at two distinct temperatures (~170 and 280 °C) during temperature ramp. Thus, H_2S adsorption at elevated temperatures produced surface sulfur by replacement of surface lattice oxygen at two types of minority sites (max. 5% of a monolayer). Therefore we suggest that multicoordinated OH groups and surface lattice oxygen at defective sites are involved. CO-TPR revealed increased reactivity of surface lattice oxygen on ZrO_2 with increasing amount of sulfur on the surface. In addition, strong adsorption of carbonates was suppressed by the presence of sulfur. The observed H_2S-induced enhancement of naphthalene oxidation in gasification gas clean-up is suggested to be caused by the increased reactivity of surface oxygen species in the vicinity of sulfur species on the surface.

1. Introduction

Syngas can be produced from biomass by gasification. The product gas can be targeted to energy, H_2, or liquid fuels production, affording a CO_2 neutral route to produce fuels. The main challenge in the utilization of product gas from biomass gasification arises because of tars (modeled as toluene and naphthalene) present in the produced syngas. Sulfur compounds, such as H_2S and COS, and ammonia are also present as impurities. The content of tar in the gas is very low, but due to its tendency to plug downstream processing equipment it has to be removed from the gas to ppb level. A competitive way to convert tars to less harmful compounds is catalytic hot-gas cleaning, which can take place inside the gasifier or in a specially designed tar removal unit [1,2]. The types of catalysts studied include metal catalysts such as nickel, alkali metals, and precious metals (Rh, Pt) [3], and e.g. dolomites [1]. ZrO_2-based catalysts are known to be active in tar decomposition when oxygen is added to the gas [4].

The level of H_2S in biomass gasification gas may be as high as 500 ppm [5], thus sulfur tolerance of the catalyst is essential. Metal catalysts are known to be poisoned severely by H_2S. Apparently, sulfur bonds so strongly to metal surfaces that marked loss of activity may occur at extremely low gas-phase concentrations [6]. For example, even 0.5–15 ppm of sulfur is enough to cause severe deactivation of conventional nickel steam reforming catalysts [7]. Sulfur tolerance of precious metals (Rh, Pt) may be somewhat higher [3]. Interestingly, studies on ZrO_2-based gasification gas clean-up catalysts have shown that H_2S may even have an enhancing effect on naphthalene conversion in catalytic hot-gas cleaning. Enhancement of naphthalene oxidation activity was observed mainly at 600 and 700 °C on pure ZrO_2 and Y_2O_3–ZrO_2, but not on SiO_2–ZrO_2. [2,3]

Other studies also report H_2S having a promoting effect in catalysis on metal oxides [8–11]. Laosiripojana et al. [8] investigated steam reforming of methane over CeO_2-based catalysts in the presence of H_2S. Their studies indicated that an appropriate amount of

* Corresponding author. Tel.: +358 50 5300129.
E-mail address: inkeri.kauppi@aalto.fi (E.I. Kauppi).

http://dx.doi.org/10.1016/j.apcatb.2014.09.042
0926-3373/

H_2S promotes the reforming activity and, moreover, the enhancement effect was connected with the formation of various Ce–O–S phases during the reaction [8]. H_2S has also been found to affect the reaction between CH_4 and CO_2 over TiO_2 and SiO_2 supported Rh-catalysts, supposedly by selective poisoning of active sites [10]. Regarding oxidation reactions, Vincent et al. [9] reported recently a strong promoting effect of H_2S on methane oxidation over sulfur resistant metal oxide catalysts (a mixture of $La_{0.4}Sr_{0.6}TiO_3$ and Y_2O_3–ZrO_2) [9].

Chemical species adsorbed on the catalyst surface affect the catalytic activity profoundly [12]. However, it is not commonly known what kind of interactions with H_2S benefit catalyst operation. While it is known that sulfate (SO_X) species affect superacidic properties of ZrO_2 promoting mainly isomerization or condensation type of reactions [12–14], it remains unclear what kind of sulfur derived surface species affect promotion of oxidation reactions on ZrO_2. Possibly, adsorption of S on ZrO_2 modifies the surface chemistry and thus the catalytic properties, or S is involved via reactions with the species to be oxidized, offering new reaction pathways.

Some studies suggest that sulfur interaction with lattice is connected with the promoting effects of H_2S on ZrO_2 [2,11]. Adsorption of H_2S induces structural changes on ZrO_2 via O^{2-} atoms being replaced by S^{2-} in the lattice, which has been estimated to increase basicity and/or redox properties of ZrO_2 [11]. It has also been reported that when O sites are replaced by S the average Zr–O distance increases resulting in increased ionicity of the Zr–O bond [15]. In addition, H_2S dissociated surface species are expected to alter the properties of ZrO_2. Travert et al. [16] observed creation of very acidic surface hydroxyl groups (and consumption of lower coordinated ones) upon H_2S dissociative adsorption on ZrO_2. H_2S dissociated species have been found to occupy Zr^{4+} sites, thus lowering the Lewis acidity of ZrO_2 [16,17]. The above mentioned H_2S-induced changes on the ZrO_2 surface affect the adsorption of reactant molecules and thus, effects on catalytic activity are observed.

Among characterization techniques to study H_2S adsorption, IR is relatively easily applied in situ and has been used to study the adsorption of H_2S on metal oxides, mainly Al_2O_3 (e.g. [18]), but also ZrO_2 (e.g. [11,16]). However, challenges arise due to the weak response of S–H in infrared. The stretching vibrations of S–H give weak IR bands due to their low extinction coefficient, and the bending vibration has even lower intensity in the region where many metal oxides are even not transparent to IR beam [16]. Regarding characterization of S in the lattice, Datta and Cavell [18] noted that it is not possible to monitor the presence of an M–S bond by infrared spectroscopy and suggested that XPS technique could be more suitably used for this purpose [18]. Sohn and Kim [12] studied modification of ZrO_2 by sulfur compounds via infrared and photoelectron spectroscopies. By XPS (ex-situ) they were only able to confirm the presence of oxidized sulfur species (S^{6+}) and they also noted that the reduced species are fully oxidized in O_2-containing atmosphere [12]. Laosiripojana et al. [8] did postreaction characterizations (XRD, XPS) on CeO_2-based reforming catalysts to study the effect of H_2S and information on sulfur-containing phases was attained. In the study it was also noted, that in situ XPS studies are needed to determine the oxidation states during reaction [8]. Such studies demand dedicated equipment due to contamination with sulfur species. Bringing the sulfided sample to ambient is thus likely to affect the amount and nature of sulfur on the surface and therefore render ex situ characterization ineffective.

Oxidation of naphthalene is thought to involve surface oxygen on ZrO_2 [2]. Thus, the aim of this work is find out how sulfur manipulates the reactivity of ZrO_2 towards oxidation reactions. Oxygen is present on the ZrO_2 surface in terminal or multicoordinated hydroxyl (t-OH, m-OH) groups and surface lattice oxygen with different level of unsaturation, i.e. on terraces and steps, kinks and defects. Temperature-programmed techniques were used to discover the effect of adsorbed H_2S on the reactivity of oxygen on ZrO_2.

2. Experimental

Monoclinic ZrO_2 from MEL Chemicals was used as catalyst. The specific surface area was 24 m^2/g (measured by BET-method), which was reported in [19] among other physical and chemical properties. The density of O-atoms on the surface of ZrO_2 was estimated to be $1.5 \cdot 10^{19}$ O/m^2, which was calculated based the density of O-atoms in the unit cell assuming that (1 0 0) faces are exposed [19,20]. The purity of ZrO_2 was studied by XPS analysis and no impurity metals were detected (except for Hf).

TP-experiments were performed using a sample of 0.1 g (particle size 0.25–0.42 mm). The catalyst powder had been pre-calcined at 800 °C for 1 h and pressed into pellets, which were crushed and sieved to the desired particle size. TP-experiments were carried out in an Altamira AMI-100 characterization system. The gaseous products were analyzed with a mass spectrometer (MS, Omnistar GSD320, Pfeiffer Vacuum).

The experiments were carried out using calcined and reduced samples. Pre-treatment of the samples was done in-situ under O_2/He (10 vol-% O_2 in He, AGA) at 600 °C for 2 h (ramp rate 10 °C/min) following reduction in 10 vol-% H_2/He (H_2 99.999%, AGA) for 15 min to mimic the state of the surface during gasification gas clean up (the concentration of reducing gases in gasification gas is high). All further treatments were done in-situ and the sample was never exposed to ambient during the TP-cycles.

2.1. Temperature-programmed sulfiding (TPS)

TPS was performed flowing 50 cm^3/min of H_2S/N_2 (500 ppm of H_2S, AGA) through the catalyst bed first at 30 °C for 0.5 h. The gas was purposely free of H_2 to prevent reduction of the surface by H_2. However, the gas mixture may have contained ppm levels of water as impurity. After initial adsorption at 30 °C, temperature was increased from 30 °C to the end temperature at a rate of 10 °C/min under similar H_2S flow. Sulfiding was continued at the end temperature for 1 h, whereafter the sample was cooled down under H_2S-containing flow. The sample was flushed with inert for 1 h at 30 °C to remove weaker held species before probing of the H_2S-treated surface.

H_2S was adsorbed on ZrO_2 isothermally at 30 °C (1 h) and via TPS at four different final temperatures of 100, 200, 300 and 400 °C aiming to affect the amount (and nature) of H_2S adsorbed species on the surface. The differently sulfided samples are designated $H_2S_{ads30\,°C}$, $TPS_{30–100–30\,°C}$, $TPS_{30–200–30\,°C}$, $TPS_{30–300–30\,°C}$ and $TPS_{30–400–30\,°C}$.

The consumption of H_2S during H_2S adsorption was calculated by numerically integrating the area of the H_2S signal compared to 500 ppm in the feed gas.

2.2. Probing the sulfided surface

The sulfided ZrO_2 surface was tested via temperature-programmed methods; temperature-programmed desorption (TPD), temperature-programmed reduction with hydrogen (H_2-TPR), and temperature-programmed reduction with CO (CO-TPR). The TPD, H_2-TPR, and CO-TPR results with sulfided ZrO_2 were compared to results obtained on unsulfided (calcined and reduced) ZrO_2 to determine the effect of adsorbed H_2S.

TPD was performed after flushing the sample at 30 °C with N_2 (50 cm^3/min, AGA, 99.999%) after $TPS_{30–400–30\,°C}$ for 1.5 h. Thereafter a temperature ramp was applied from 30 to 600 °C under similar N_2 flow (10 °C/min).

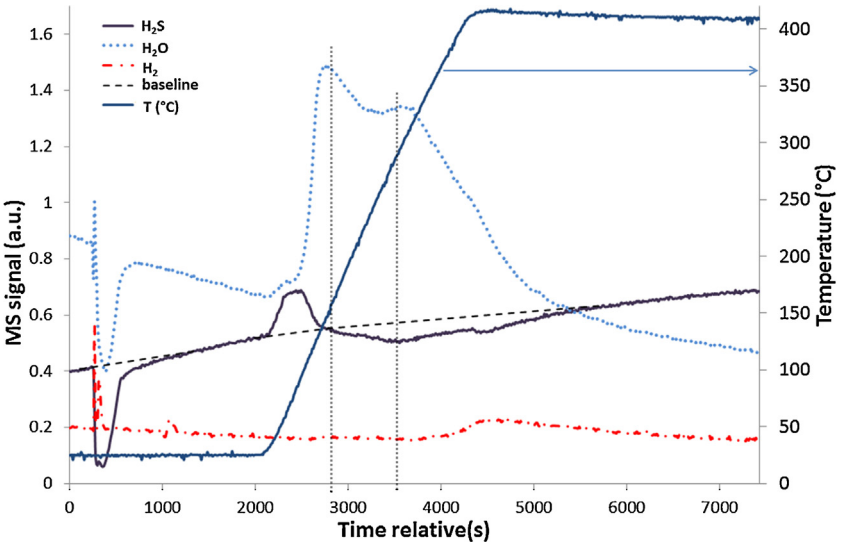

Fig. 1. TPS profile (MS signals for H_2S, H_2O, and H_2) from 30 to 400 °C on ZrO_2 (500 ppm H_2S in N_2). In the figure also the isothermal adsorption stage at 30 °C (0.5 h) is shown.

H_2-TPR was performed after $TPS_{30–400–30\,°C}$. A gas mixture of H_2/N_2 (50 cm^3/min, 4 vol-% H_2) was admitted to the reactor at 30 °C and let to dwell for 0.5 h. Then, a temperature ramp was applied under H_2-containing flow from 30 to 600 °C (10 °C/min) and the end temperature was maintained for 0.5 h.

CO-TPR was performed after 1 h He flush (50 cm^3/min, AGA, 99.996%) at 30 °C on the five differently sulfided ZrO_2 samples described before. A total flow of 50 cm^3/min CO in He (5 vol-% CO) was passed through the samples first at 30 °C for 0.5 h and during ramp from 30 to 600 °C (10 °C/min). The sample was let to dwell at 600 °C for 0.5 h.

The gas phase products were analyzed by MS. Compounds analyzed and their respective m/z values monitored during TPD and H_2-TPR runs were H_2, (m/z = 2), He (m/z = 4), water (m/z = 18), H_2S (m/z = 34, 33, and 32), CO or N_2 (m/z = 28), CO_2 (m/z = 44) and SO_2 (m/z = 64 and 48). During CO-TPR, the production of any possible sulfided products from CO were also monitored (methanethiol, COS and CS_2, m/z = 45, m/z = 60, and m/z = 76, respectively). For calibrating the MS, one point calibration with constant feed was used (for H_2S 500 ppm H_2S/N_2, and for CO_2 1 vol-% CO_2/He).

3. Results

3.1. Sulfiding of ZrO_2

Temperature-programmed sulfiding (TPS) of the catalysts was carried out to gain information about H_2S adsorption sites and sulfur binding on the ZrO_2 surface.

H_2S was adsorbed on pre-reduced ZrO_2 isothermally at 30 °C and via TPS from ambient temperature to 100, 200, 300 and 400 °C. Fig. 1 shows the result of a TPS run with end temperature of 400 °C, where the dotted line indicates the baseline of the H_2S signal (based on a blank experiment), used to calculate the amounts of H_2S that adsorb and desorb at different stages of the temperature program. The results of TPS runs with final temperatures 100, 200, and 300 °C are presented in supplementary information in Figs. S1, S2, and S3, respectively. The signal m/z = 34 is shown for H_2S and also the signals m/z = 33 and m/z = 32 for SH^- and S^{2-} showed similar profiles. H_2S was consumed immediately at 30 °C when it was introduced into the reactor, which can be seen in Fig. 1 between 240 and 1000 s. When a temperature ramp was applied at approx. 2050 s, H_2S desorbed with a maximum at 55 °C with minor formation of water. This was similar in all the experiments (shown in S1, S2, and S3). During temperature ramp from 30 to 400 °C, H_2S was consumed at approx. 170 and 280 °C with concurrent formation of water (temperatures corresponding roughly to H_2O production and H_2S consumption maxima, Fig. 1). The same processes took place during $TPS_{30–300–30\,°C}$ as can be seen in Fig. S3 during temperature ramp. Simultaneous H_2S consumption and H_2O production was also seen during TPS experiments until 100 and 200 °C (Figs. S1 and S2). The peak areas for desorbing water during ramp were calculated and correlated with adsorbing H_2S amounts, to confirm the relevance of the results. Their linear correlation is shown in S4. H_2S was also consumed during cooling, similarly for all experiments (not shown). The multiple processes for H_2S consumption indicate that at least three types of sites exist to adsorb H_2S on the ZrO_2 surface. Apparently two of these sites are able to release oxygen, since separate maxima for water were detected concurrently with H_2S consumption.

Finally, H_2S adsorbed at approx. 400 °C with simultaneous formation of H_2 in Fig. 1 (the amount of H_2 being 0.26 μmol) indicating that at this temperature H_2S started to decompose forming H_2 (no significant H_2 signal was detected in all other experiments in Figs. S1–S3). Experiments with an empty reactor showed that this does not occur without a catalyst. It was also noted, that H_2 was produced (exponential increase with H_2S consumption) during TPS until 600 °C, also suggesting decomposition of H_2S rather than surface reaction. It is thought that under the reducing conditions of gasification gas clean-up elemental sulfur is not formed (other components in the gas mixture are likely to stabilize H_2S [21]), and therefore the maximum temperature in TPS experiments was limited to 400 °C.

Table 1 shows the amounts of H_2S adsorbed during the TPS experiments and the estimations of respective monolayer coverage (%, calculated as amount of H_2S per number of O atoms on the surface of ZrO_2 sample). The "sum" indicates the amount that was retained on the catalyst, based on the cumulative amounts that were adsorbed, subtracting the amount that desorbed. The amount of H_2S adsorbed at 30 °C was reproducible 3.5 μmol, corresponding to approx. 6% of a monolayer, in all experiments (Table 1). Approximately half of this amount was desorbed during temperature ramp at 55 °C (Table 1), which can be attributed to desorption of physisorbed H_2S. The amount of H_2S adsorbed during cooling was similar, so apparently the process is reversible as would be expected for physisorption. Minor amounts of water also desorbed right after heating was started. The amount of adsorbed

Table 1
Calculated amounts (μmol) of adsorbed and desorbed H_2S during adsorption at 30 °C and TPS runs at varied final temperatures on 0.1 g ZrO_2. Value in parentheses indicates the ML amount (% of surface coverage).

	$H_2S_{ads30\,°C}$	$TPS_{30–100–30\,°C}$	$TPS_{30–200–30\,°C}$	$TPS_{30–300–30\,°C}$	$TPS_{30–400–30\,°C}$
At 30 °C	3.5 (5.8)	3.6 (6)	3.5 (6)	3.5 (6)	3.5 (5.9)
Desorption during ramp	–	1.7 (2.9)	1.7 (2.8)	1.7 (2.9)	1.7 (2.8)
Activated adsorption	–	0.4 (0.7)	1.4 (2.3)	2.6 (4.3)	3.2 (5.4)
Adsorption during cooling	–	1.2 (2)	1.8 (3)	1.6 (2.8)	1.6 (2.6)
Sum	3.5 (5.8)	3.5 (5.9)	4.7 (8.6)	6.0 (10.1)	6.5 (11)

H_2S species increased from 0.4 to 3.2 μmol by increasing sulfidation end temperature from 100 to 400 °C (Table 1), indicating that H_2S adsorption was activated with temperature (adsorption at elevated temperatures will therefore be denoted activated adsorption). However, the increase was less significant when the end temperature was increased from 300 to 400 °C, at which temperature H_2S started to decompose to H_2 and S. Therefore, sulfidation capacity is apparently saturating around 400 °C.

TPS with end temperature of 400 °C was also performed on pre-treated and wetted catalyst (a flow of 50 cm^3/min H_2O/He, 1000 ppm, was passed through the catalyst at 30 °C for 0.5 h and thereafter flushed for 0.5 h prior to TPS). Wetting the catalyst only suppressed H_2S adsorption at low temperatures (30 °C), whereas at higher temperatures, after additional H_2O had desorbed, the adsorption pattern was similar compared to that on the reduced catalyst (not shown). The results indicated that the amount of physisorbed H_2S was decreased by molecularly adsorbed water on the catalyst.

3.2. Reactivity of sulfided ZrO_2

3.2.1. TPD and H_2-TPR; thermal stability and reactivity towards H_2

TPD and H_2-TPR were performed on unsulfided ZrO_2 and after $TPS_{30–400–30\,°C}$. The results from both experiments will be presented and discussed together in order to describe the effect of sulfidation on the properties of ZrO_2. Fig. 2A shows H_2S desorption during TPD on unsulfided ZrO_2 and ZrO_2 after $TPS_{30–400–30\,°C}$. As can be seen, H_2S desorbs from the sulfided sample with a sharp maximum at 80 °C, which can be connected with residual molecularly adsorbed H_2S. Desorption of weakly held species was also seen during TPS (Fig. 1) after heating was started. In the beginning of the temperature ramp during TPD (Fig. 2B) the signal for water rises indicating that some molecular water was also present. Fig. 3 shows the results of H_2-TPR experiments on unsulfided and sulfided ZrO_2. The sulfided sample shows a maximum for H_2S at approx. 75 °C corresponding to low temperature H_2S desorption during TPD and can therefore be assigned to desorption of residual molecular H_2S. Also water desorbed at low temperature after heating was started (Fig. 3B) which is assigned to molecularly adsorbed water.

A broad maximum for desorbing H_2S was observed in Fig. 2A also at approx. 300 °C during TPD after $TPS_{30–400–30\,°C}$. Based on earlier H_2S-TPD studies on ZrO_2 catalysts, when H_2S was adsorbed isothermally at 40 °C, only one peak for desorbing H_2S was detected (maximum at 100 °C) [17]. Therefore it is proposed that, the H_2S species that desorb at approx. 300 °C after $TPS_{30–400–30\,°C}$ result from surface species formed via an activated process. Water desorbed during TPD on the unsulfided ZrO_2 with a maximum at 360 °C (Fig. 2B), whereas the sulfided ZrO_2 (via $TPS_{30–400–30\,°C}$) hardly showed any H_2O desorption. Particularly it can be seen that the peak at approx. 360 °C in Fig. 2B, which is attributed to dehydroxylation of ZrO_2 [22–24], was diminished on the sulfided sample. Apparently there are less hydroxyl groups that are able to react to water on the sulfided surface. It is thus suggested that H_2S adsorption titrated hydroxyl groups on the surface, which is in line with data from Travert et al. [16].

During H_2-TPR on the sulfided sample a sharp maximum for H_2S appeared at approx. 320 °C with simultaneous formation of H_2O and consumption of H_2 (Fig. 3). The amount of H_2S formed at 320 °C was calculated to be 2.5 μmol and that of H_2O 6 μmol for the peak at 320 °C, based on rough estimation. On the other hand, H_2 consumption was calculated to be 11.4 μmol. The sulfided sample also showed a maximum for water at 375 °C. It is probable that part of the H_2 is consumed in this process (reduction of surface oxygen species), since the amount of H_2 consumed is higher than the calculated molar amounts of H_2S and H_2O formed at 320 °C. On the unsulfided sample water was formed during H_2-TPR at 350 °C (Fig. 3B) which is suggested to originate from dehydroxylation, similarly as during the TPD experiments. Furthermore, the consumption of H_2 on the unsulfided ZrO_2 was zero, since no clear change was observed in the H_2 curve (ZrO_2 is not reducible below 600 °C). Only the sulfided sample showed a distinct minimum in the H_2 curve (320 °C, Fig. 3C) indicating consumption of hydrogen. No SO_2 formation was detected on the sulfided samples during TPD nor H_2-TPR suggesting that ZrO_2, unlike e.g. TiO_2 [10,25], is not able to provide oxygen to form SO_2.

The amount of desorbing H_2S during TPD was calculated to be 2.1 μmol, corresponding to 29% of the total amount of H_2S that was present on the surface after $TPS_{30–400–30\,°C}$. The total amount of H_2S desorbed during H_2-TPR corresponds to 53% of the total amount of H_2S that was left on the surface after TPS.

An additional temperature-programmed oxidation experiment was performed after TPD to check if any S species remained on the surface after TPD. The results showed SO_2 formation at room temperature right after O_2/He (10 vol-%) feed was started, so evidently sulfur species remained which are easily oxidized at room temperature.

3.2.2. CO-TPR on sulfided vs. unsulfided ZrO_2

The surfaces sulfided to different extent ($H_2S_{ads30\,°C}$, $TPS_{30–100–30\,°C}$, $TPS_{30–200–30\,°C}$, $TPS_{30–300–30\,°C}$ and $TPS_{30–400–30\,°C}$) were studied in CO-TPR in order to determine the reactivity of the catalysts towards CO.

Fig. 4A and B show CO_2, H_2S, H_2O and H_2 generation during CO-TPR experiment on unsulfided and sulfided ZrO_2 ($TPS_{30–400–30\,°C}$). CO consumption cannot be reported because of a too low signal to noise ratio. Fig. 4A and B show that H_2O desorbs from the unsulfided ZrO_2 showing no significant maxima, whereas maxima are seen on the sulfided ZrO_2 at approx. 190 and 380 °C. CO was not found to react directly with adsorbed H_2S on the sulfided surface, i.e. no products containing C and S could be detected with MS. On the other hand, it is possible that if such products were formed they were retained on the surface even after 600 °C. Remarkably, the sulfided ZrO_2 ($TPS_{30–400–30\,°C}$) clearly shows an additional peak for CO_2 at low temperature (190 °C) in Fig. 4B as compared to unsulfided sample in Fig. 4A, for which only one CO_2 peak is detected at high temperature, concurrently with a H_2 peak. Instead the low-temperature generation of CO_2 occurs with simultaneous formation of H_2S and H_2O. H_2 was generated simultaneously with CO_2 having maxima at 480 and 535 °C on unsulfided and sulfided ZrO_2, respectively.

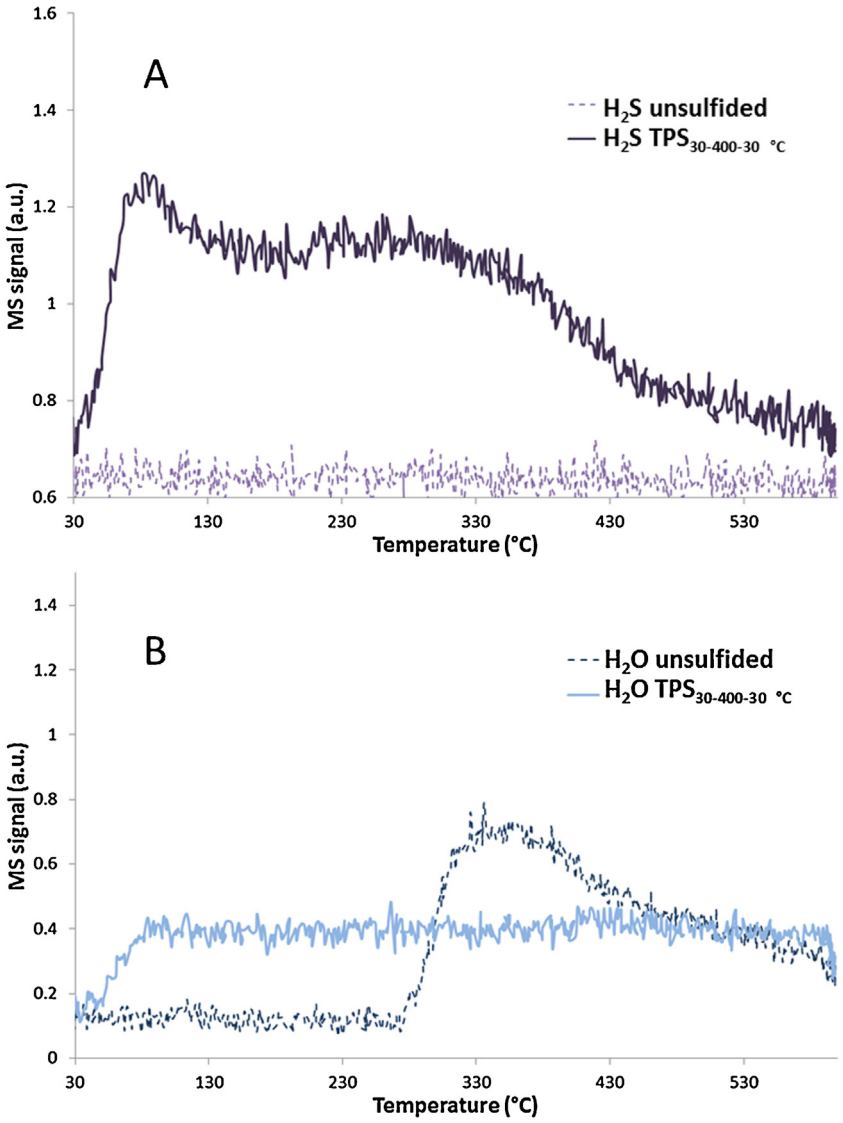

Fig. 2. MS signal for A) H_2S (m/z = 34) and B) H_2O (m/z = 18) during TPD from 30 to 600 °C (ramp rate 10 °C/min) on unsulfided and sulfided ZrO_2 (via $TPS_{30–400–30\,°C}$).

Table 2 shows temperatures at which maxima were detected for CO_2, H_2O, H_2 and H_2S on unsulfided and differently sulfided ZrO_2 samples. CO_2 and H_2 are generated at high temperature (~530 °C) on all the sulfided ZrO_2 samples, corresponding maxima are seen on the unsulfided ZrO_2 at 480 °C. The additional maximum for CO_2 at 190 °C is seen on all the sulfided catalysts. The intensity of the peak clearly increases with increasing sulfidation temperature and on the sample sulfided at 30 °C this is barely noticeable (Fig. 5). Minor amounts of water desorbed during the CO-TPR experiments on all the catalysts. H_2S desorbed at 190 °C after $TPS_{30–200–30\,°C}$, $TPS_{30–300–30\,°C}$, and $TPS_{30–400–30\,°C}$.

The amounts of CO_2 generated on unsulfided and differently sulfided ZrO_2 as shown in Fig. 5 are presented in Table 3. The total amount of oxygen atoms removed from the ZrO_2 surface by CO oxidation was no more than 5% of a ML (% of the total number of oxygen atoms in one monolayer on the ZrO_2 surface). It can be seen that increasing the sulfiding temperature (and therefore the amount of activatedly adsorbed species) caused an increase in the amount of the CO_2 produced at 190 °C as already discussed above. On the other hand, H_2S adsorption isothermally at 30 °C and via TPS at 100 °C produced additional high temperature CO_2 maxima at 500 and 440 °C, respectively, during subsequent CO-TPR (Fig. 5). These appeared without simultaneous H_2 production. H_2S treatment causes the amount of CO_2 to increase, independent of the end temperature of TPS.

The possible presence of sulfate (SO_X) species was considered to affect the differing properties of ZrO_2 after sulfidation and thus the CO-TPR experiment was performed also on sulfated ZrO_2 (ZrO_2

Table 2
CO_2, H_2O, H_2 and H_2S (m/z = 44, 18, 2 and 34, respectively) maxima (°C) at unsulfided and differently sulfided ZrO_2 surfaces during CO-TPR (5 vol-% CO).

	Unsulfided	$H_2S_{ads30\,°C}$	$TPS_{30–100–30\,°C}$	$TPS_{30–200–30\,°C}$	$TPS_{30–300–30\,°C}$	$TPS_{30–400–30\,°C}$
CO_2	480	(190), 500, 530	190, 440, 530	190, (315, 425), 535	190, (310, 390), 535	190, (260, 390), 535
H_2O	170, 250, 360	60, 350	70, 180, 290, 370	75, 175, (300, 475)	70, 170, 390	(80), 180, (390)
H_2	480	530	530	535	535	535
H_2S	–	–	–	190	190	(80), 190

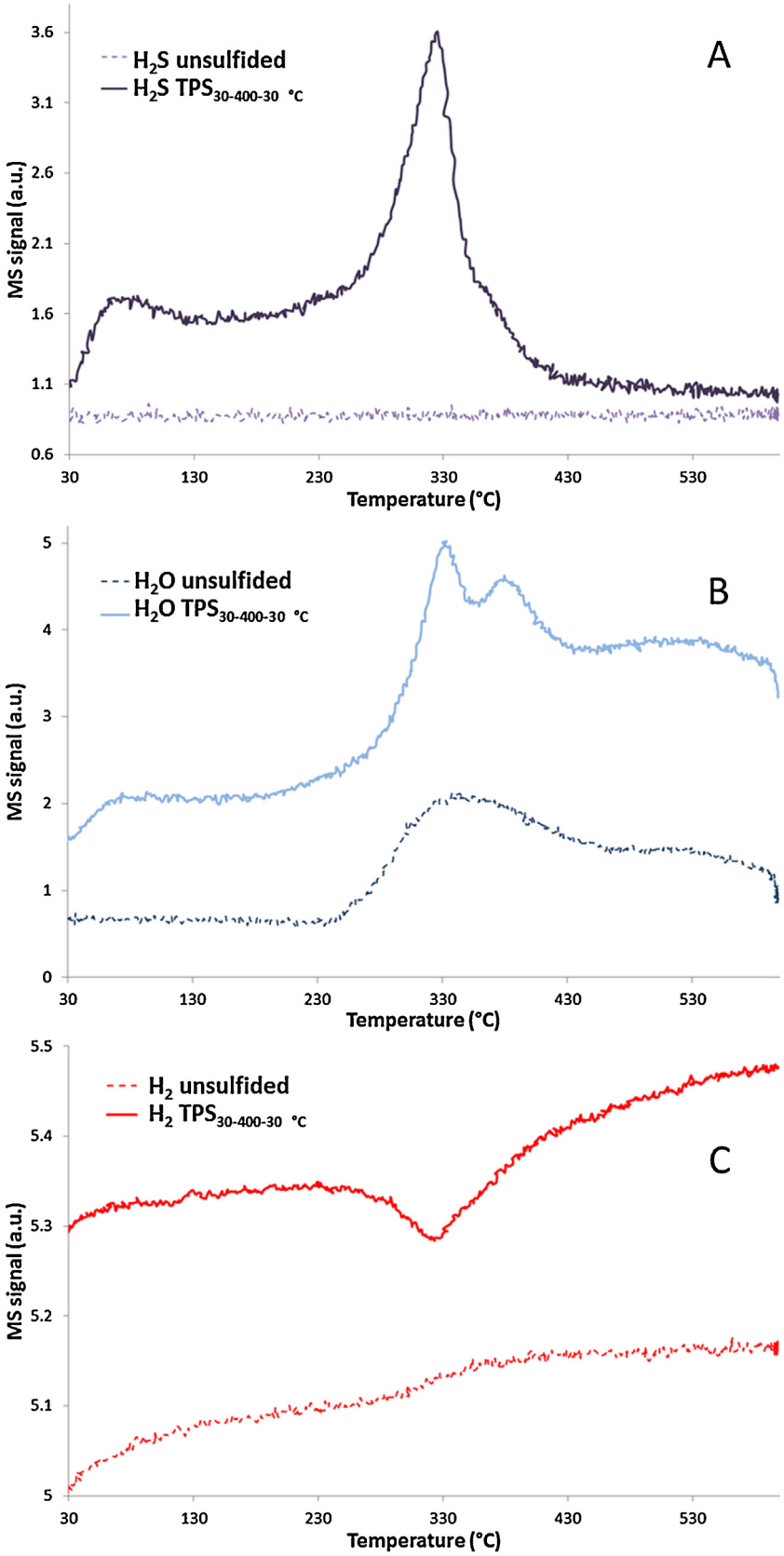

Fig. 3. MS signal for (A) H_2S ($m/z = 34$), (B) H_2O ($m/z = 18$), and (C) H_2 ($m/z = 2$) during H_2-TPR from 30 to 600 °C (ramp rate 10 °C/min) on unsulfided and sulfided ZrO_2 (via $TPS_{30–400–30\,°C}$).

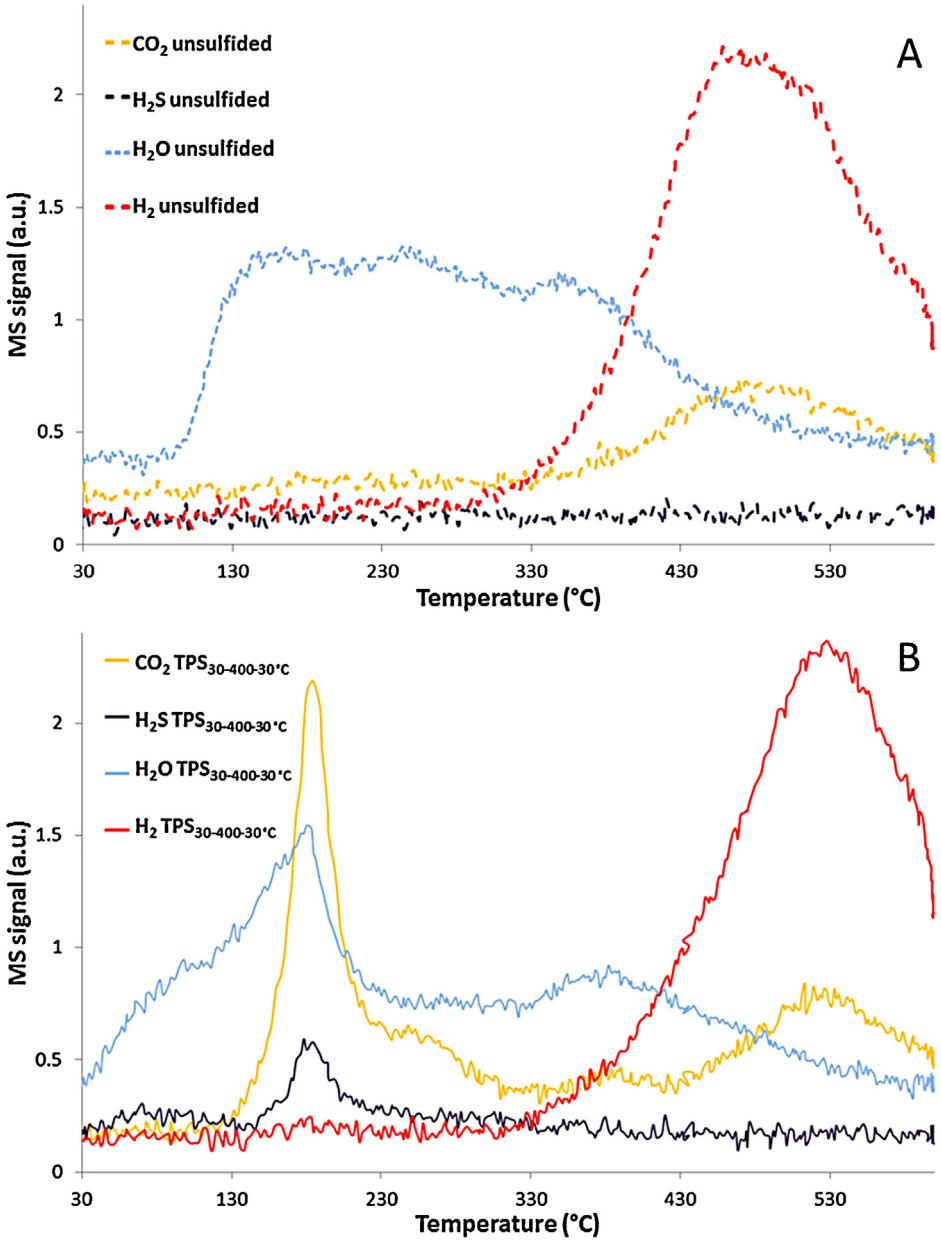

Fig. 4. Formation of CO_2, H_2S, H_2O and H_2 (MS signals m/z = 44, 34, 18 and 2, respectively) during CO-TPR on (A) unsulfided and (B) sulfided via $TPS_{30–400–30\,^{\circ}C}$ ZrO_2.

treated with H_2SO_4). The results showed CO_2 formation with simultaneous release of SO_2 at 570 °C, a temperature which is consistent with literature [26]. Therefore it is evident that the interaction of sulfided zirconia with CO is not related to the presence of any sulfates on the surface.

4. Discussion

This discussion concentrates on how H_2S adsorption modifies the surface of monoclinic ZrO_2 and how these modifications affect the reactivity of surface oxygen. By surface oxygen we mean terminal or multi-coordinated hydroxyls on the surface (t-OH, m-OH) and surface lattice oxygen with different level of unsaturation, i.e. on terraces as well as defective sites. Products evolved during H_2-TPR and CO-TPR on samples sulfided to different degree provide information on the ability of the surface to supply oxygen for oxidation reactions and indirectly on possible sulfur surface species that induce these changes. CO-TPR results showed that adsorbed sulfur species do not form any gas-phase products with CO in the studied temperature range. This confirms that the effects discussed

Table 3
Amount of CO_2 generated (μmol) during CO-TPR on unsulfided and differently sulfided catalysts. The value in parentheses indicates the quantity of oxygen removed from the ZrO_2 surface (% of a ML).

CO_2 (μmol)	Unsulfided	$H_2S_{ads30\,^{\circ}C}$	$TPS_{30–100–30\,^{\circ}C}$	$TPS_{30–200–30\,^{\circ}C}$	$TPS_{30–300–30\,^{\circ}C}$	$TPS_{30–400–30\,^{\circ}C}$
~190 °C	0 (0)	0.3 (0.3)	0.9 (0.7)	1.6 (1.4)	2.6 (2.2)	2.9 (2.4)
~500 °C	2.7 (2.3)	4.0 (3.4)	3.7 (3.1)	2.2 (1.9)	2.1 (1.8)	2.1 (1.8)
Tot	2.7 (2.3)	4.3 (3.7)	4.9 (4.1)	5.5 (4.6)	6.1 (5.1)	6.2 (5.2)

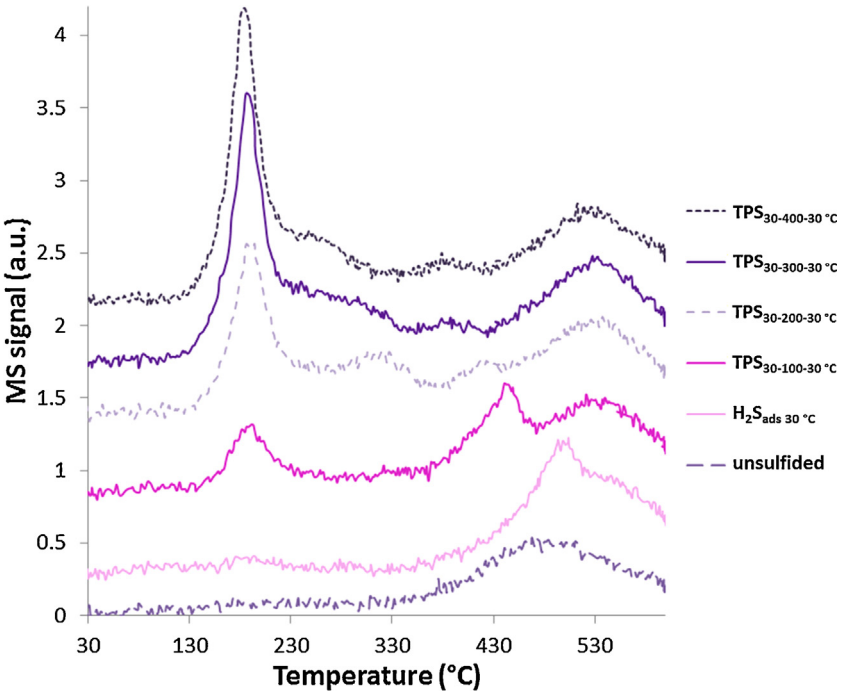

Fig. 5. CO_2 generation on unsulfided and differently sulfided ZrO_2 during CO-TPR from 30 to 600 °C (10 °C/min, 5 vol-% CO in He).

below are due to incorporation of S in ZrO_2, instead of opening new reaction pathways via S-containing intermediates.

4.1. H_2S adsorption on ZrO_2

H_2S was adsorbed isothermally on ZrO_2 at 30 °C and in a temperature-programmed mode from 30 to 100, 200, 300 and 400 °C. Approximately half of the H_2S adsorbed isothermally at 30 °C was physisorbed and relatively easily removed from the surface at 55 °C (the instability of physisorbed H_2S has been indicated also earlier [17,18]). This process is reversible since the amount adsorbed during cooling corresponds to the physisorbed amount (Table 1). Desorption of the weakly held, physisorbed H_2S was seen during TP-treatments on the sulfided catalysts in the initial part of the temperature ramp (TPD, H_2-TPR and CO-TPR in Figs. 2A, 3A, and 4B, respectively). Molecularly adsorbed water on the surface seems to hinder the adsorption of physisorbed H_2S, based on the TPS result on wetted surface (not shown).

In addition to physisorbed H_2S, half of the H_2S species adsorbed at 30 °C were retained on the surface when heating was started during TPS (Table 1). Catalyst properties were affected even after isothermal adsorption at 30 °C (as observed with CO-TPR, Fig. 5), confirming H_2S dissociation and formation of stable surface species, even at this low temperature. Travert et al. studied H_2S and CH_3SH adsorption on metal oxides, including ZrO_2, by FTIR [16]. They observed disappearance of original high frequency ν(OH) band and increase and shift of the low-frequency ν(OH) band. At the same time a broad band accompanied with a bending HOH vibration was observed. Weak bands for SH were also observed at low temperature. [16] Thus, dissociation of H_2S at low temperature occurs on terminal hydroxyl (t-OH) groups (Eq. 1) and coordinatively unsaturated surface oxygen anions (O^{2-}) generating new multicoordinated hydroxyl (m-OH) groups and SH groups (Eq. 2).

$$\text{t-OH(s)} + H_2S(g) \rightarrow H_2O(g) + \text{SH(s)} \quad (1)$$

$$O^{2-}(s) + H_2S(g) \rightarrow \text{m-OH(s)} + \text{SH(s)} \quad (2)$$

Water desorbed in the beginning of the temperature ramp during the TPS experiments (Fig. 1). TPD results after $TPS_{30–400–30\,°C}$ showed desorption of minor amounts of water, and the water peak corresponding to dehydroxylation at 340 °C (Fig. 2B) was nonexistent. Dehydroxylation involves t-OH and m-OH groups [22–24], so it is suggested that at 30 °C H_2S dissociated, titrating terminal hydroxyl groups on the surface via Reaction 1. H_2S may also dissociate via Reaction 2 forming new m-OH groups.

Activated H_2S uptake took place during TPS, generating water at two different temperatures (~170 and 280 °C, Fig. 1), suggesting reaction with surface oxygen. It has been proposed that several metal oxides, including ZrO_2, are able to exchange surface lattice oxygen with S from adsorbing H_2S via following reaction $H_2S + O^{2-}{}_{surf.} \rightarrow H_2O + S^{2-}{}_{surf.}$ [11,25,27–29]. Ziolek et al. [11] suggested that this affects increase of basicity or redox properties on ZrO_2. For ZrO_2, the surface oxygen sites available for this type of exchange would be, in principle, m-OH groups, surface lattice oxygen at terraces, or surface lattice oxygen at edges or low coordination sites. The observation that the maximal amount of H_2S adsorbed is in the order of 5% of a ML (Table 1), is suggesting that minority sites, i.e. defective sites, are involved instead of oxygen at terraces. Therefore we suggest that TPS-induced incorporation of sulfur on the surface is replacing oxygen at m-OH groups at lower temperature (170 °C) and surface lattice oxygen at low coordination sites at the higher end of the temperature ramp. Sulfur in the lattice might also result via an activated conversion of –SH groups formed via H_2S dissociated at lower temperatures. According to Beck et al. [25], H_2S exposure to TiO_2 (rutile) above 350 °C forms mostly strongly bound sulfide species which can remain on the surface or diffuse into the lattice [25]. Also in our study, diffusion of sulfide (S^{2-}) into the bulk lattice cannot be completely excluded.

The H_2S uptake leveled off between 300 and 400 °C. Also H_2S decomposition started at temperatures above 360 °C resulting in deposition of elemental S, based on the occurrence of H_2 generation in Fig. 1. It is known that bulk sulfide (ZrS_2) does not form upon exposure to H_2S [30], which is also consistent with the small amounts of H_2S adsorbed during TPS experiments. In principle, XRD could provide information on structure modifications by sulfur.

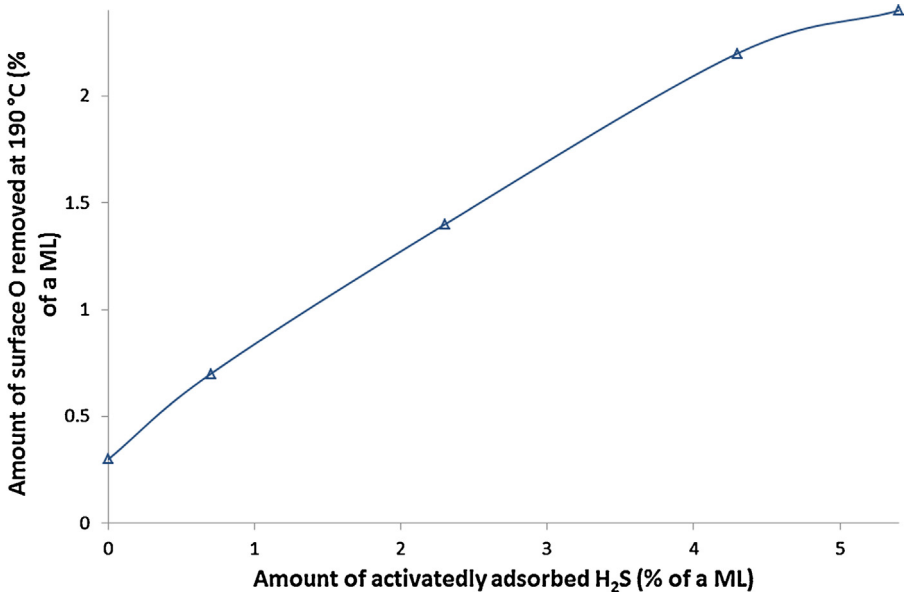

Fig. 6. Relationship between surface sulfur content of ZrO_2 and the amount of surface oxygen removed by CO oxidation at approx. 190 °C during CO-TPR on differently sulfided catalysts.

However, the amount of sulfur deposited on the surface calculated by integration of the TPS profiles was showing sub-monolayer quantities of adsorbed H_2S predicting that only specific sites on ZrO_2 surface are interacting. Since no bulk effects are expected, also XRD characterization of the sulfided ZrO_2 material is unlikely to reveal any distortions in bond lengths and so to give any additional information.

4.2. Stability of adsorbed species

According to mass balances during TPD and H_2-TPR experiments only approximately 30% of the retained H_2S desorbed and 50% could be removed by H_2. Thus, the adsorbed S species are highly stable under reducing conditions, suggesting very strong adsorption. In contrast, presence of oxygen would result in removal via SO_X formation even at mild temperatures, confirming that any ex-situ characterization including exposure to ambient cannot provide further insight.

Water desorption maxima during H_2-TPR (Fig. 3) and TPD (Fig. 2) on unsulfided ZrO_2 were very similar (350 and 340 °C, respectively). In line with this, no H_2 consumption was detected, indicating that unsulfided ZrO_2 does not contain any reducible surface oxygen species. In contrast, H_2 consumption was detected at 320 °C on sulfided ZrO_2, along with H_2S and H_2O production. Additional H_2O was produced on the sulfided ZrO_2 also at 375 °C. Furthermore, a significantly smaller dehydroxylation peak is observed on the sulfided sample in TPD (Fig. 2). Thus, water formation during H_2-TPR is significantly enhanced on sulfided ZrO_2. Simultaneous production of H_2S and H_2O at 320 °C can be attributed to reaction between dissociated H_2 (via Reaction 3) and neighboring SH and OH groups (Reactions 4 and 5, respectively).

$$H_2(g) + 2*(s) \rightarrow 2H*(s) \quad (3)$$

$$H*(s) + SH(s) \rightarrow H_2S(g) + *(s) \quad (4)$$

$$H*(s) + OH(s) \rightarrow H_2O(g) + *(s) \quad (5)$$

Since H_2S and H_2O are produced in the gas-phase simultaneously when H_2 is adsorbed, its dissociation (Reaction 3) must be the rate-limiting step.

It should be noted that during (and after) the TPD and H_2-TPR experiments the sample still contain S, which probably is responsible for the enhanced reducibility of the sample. Anderson et al. [15], suggested that S incorporated in the ZrO_2 lattice decreases the Zr–O bond strength since the volume of the unit cell increases. Therefore it is considered, that the reactive oxygen species are present in the lattice, probably at the surface. Alternatively, it may be argued that surface m-OH, which otherwise would not be reducible, are being destabilized by the presence of S.

4.3. Reactivity of oxygen on sulfided ZrO_2

Unmodified ZrO_2 is known to bind CO molecularly on surface Zr cationic sites [22,24] and as stable formates on terminal hydroxyls via an activated equilibrium process (Eq. (6) describes formate formation) [31–33].

$$CO + Zr{-}OH \leftrightarrow Zr{-}HCOO \quad (6)$$

Molecular CO desorbs already below 200 °C. Decomposition of formate occurs under CO atmosphere by 500 °C yielding CO_2 and H_2 in the gas phase [22,31,34,35], whereas in the absence of CO formate decomposes to CO and terminal hydroxyls as Reaction 6 is an equilibrium reaction. In this study CO_2 and H_2 were detected on unsulfided ZrO_2 at 480 °C during CO-TPR, whereas these maxima were shifted to approx. 530 °C after all the sulfidation treatments (Table 3). Simultaneous generation of CO_2 and H_2 is attributed to decomposition of formate, reducing the ZrO_2 surface (reductive decomposition). The formation of formates requires (terminal) hydroxyl groups [33,34] whereas their reductive decomposition requires additionally m-OH [36]. The higher temperature of formate decomposition on the sulfided surfaces indicates higher stability of formate on those catalysts or, alternatively shortage of t-OH and/or m-OH since they react with H_2S as discussed above.

Additional CO_2 formation, without concurrent formation of any other product, was seen at 500 and 440 °C on ZrO_2 after isothermal H_2S adsorption at 30 °C and after $TPS_{30–100–30\,°C}$, respectively (Fig. 5). CO_2 can be formed via decomposition of surface carbonate (bidentate or monodentate) [32,34], which are formed on the surface via reaction of CO with surface lattice oxygen and decompose at temperatures above 300 °C [31,32,34]. Thus, additional

generation of CO_2 on the ZrO_2 samples after H_2S adsorption at 30 °C or $TPS_{30–100–30\,°C}$ may be caused by CO reacting with surface oxygen during CO-TPR. We propose that the reactivity of the zirconia is modified by the presence of sulfur species adsorbed at low temperature (possibly SH species), very similar to as observed with H_2-TPR, discussed above. The formed CO_2 is retained on the surface as monodentate or polydentate carbonates, which are known to be the most stable form of adsorbed CO_2 and are also adsorbed on c.u.s. O^{2-} centers [19,37,38] (i.e. surface lattice oxygen at defects). The decrease of CO_2 desorption temperature on increasing the sulfidation degree ($TPS_{30–100–30\,°C}$ compared to $H_2S_{ads30\,°C}$) is suggested to be due to the increasing concentration of sulfur species on the surface.

Sulfiding at elevated temperatures caused a new low-temperature (~190 °C) CO_2 maximum during subsequent CO-TPR (Fig. 5). The amount of oxygen removed by CO oxidation at this temperature (Table 3) increased with the amount of activatedly adsorbed H_2S (Table 1) and a reasonable linear correlation is presented in Fig. 6. The slightly nonlinear end of the curve confirms that H_2S adsorption via this activated process (amount of surface sulfur) saturated after TPS at 300 °C and H_2S decomposition to elemental S started when further increasing temperature. The activatedly adsorbed H_2S species are very strongly bound on the surface by replacing O^{2-} by S^{2-} at low coordination sites. Therefore, increasing sulfidation temperature creates more lattice sulfur that increasingly destabilizes oxygen in the surface, enhancing the reactivity with CO. The same effect was observed during H_2-TPR, as surface oxygen species became reactive towards H_2 (see Fig. 3). Additionally, the low temperature of CO_2 desorption indicates that the sites where CO_2 adsorbs as mono/bidentate carbonate are blocked on the sulfided surface.

Naphthalene oxidation is expected to involve surface oxygen (the mechanism has been suggested to follow the Mars–van Krevelen mechanism [39]), so it is probable that its enhancement in the presence of H_2S is connected with the pronounced reactivity of surface oxygen on the sulfur-containing surface. Thus, the observed effects of H_2S on ZrO_2 can explain the reasons for naphthalene oxidation enhancement in the presence of H_2S during gasification gas clean-up. The study of Rönkkönen et al. [2] suggested that enhancement of naphthalene conversion was also connected to an adsorbed form of sulfur on the surface, since the effect remained after H_2S was removed from the atmosphere [2]. It is thought that under reducing conditions of the gasification gas-mixture the nature of sulfur compounds on the catalyst surface would be similar to the surface species in this study. Therefore, the effect is suggested to be caused by sulfur surface species that have replaced surface oxygen on ZrO_2 and enhance reactivity of surface lattice oxygen.

5. Conclusions

Temperature-programmed sulfiding study on ZrO_2 showed that at low temperature half of the H_2S adsorbed can be attributed to physisorbed H_2S, which is weakly adsorbed and leaves the surface when heating. The other half dissociates titrating terminal OH groups on the surface. The dissociated H_2S at 30 °C was also found to be strongly adsorbed. It is concluded that sulfur exchanges with surface oxygen in activated processes based on water formation at two distinct temperatures (~170 and 280 °C) during TPS until 400 °C. It is suggested that sulfur replaces oxygen at lower temperature with m-OH sites and at higher temperature with surface lattice oxygen at defective sites (minority sites). Minority sites on ZrO_2 surface are able to bind sulfur more preferably than oxygen, and moreover, sulfur adsorption on these sites enhances reactivity of surface lattice oxygen. Sulfur on the surface increased reactivity of surface lattice oxygen (reducibility of the surface) with increasing amount of surface sulfur. In addition, H_2S was found to block CO_2 adsorption sites, i.e. sites for carbonate formation, on ZrO_2. It is suggested that the observed enhancement of oxidation reactions during gasification gas clean-up is connected with increased reactivity of surface oxygen on sulfided ZrO_2 surfaces.

Acknowledgments

The authors thank Prof. Outi Krause for critical reading of the manuscript and fruitful discussions. Ms. Sonja Kouva, Ms. Ella Rönkkönen, and Ms. Tiia Viinikainen are also warmly thanked for inspiring discussions. Ms. Heidi Meriö-Talvio is acknowledged for assistance during experimental work. MEL Chemicals is thanked for donating the zirconia samples. Financing from the Ministry of Education of Finland and the Academy of Finland are gratefully acknowledged. The Finland Distinguished Professor Programme (FiDiPro) funded by the Finnish Funding Agency for Technology and Innovation (TEKES) is acknowledged for financial support.

Appendix A. Supplementary data

Supplementary material related to this article can be found, in the online version, at http://dx.doi.org/10.1016/j.apcatb.2014.09.042.

References

[1] P. Simell, E. Kurkela, P. Ståhlberg, J. Hepola, Catal. Today 27 (1996) 55–62.
[2] H. Rönkkönen, P. Simell, M. Reinikainen, O. Krause, Top. Catal. 52 (2009) 1070–1078.
[3] H. Rönkkönen, P. Simell, M. Niemelä, O. Krause, Fuel Process. Technol. 92 (2011) 1881–1889.
[4] S. Juutilainen, P. Simell, O. Krause, Appl. Catal. A 62 (2006) 86.
[5] W. Torres, S.S. Pansare, J.G. Goodwin, Catal. Rev. Sci. Eng. 49 (2007) 407–456.
[6] C.H. Bartholomew, P.K. Agrawal, J.R. Katzer, Adv. Catal. 31 (1982) 135–242.
[7] J.R. Rostrup-Nielsen, in: J.R. Anderson, M. Boudart (Eds.), Catalysis, Science and Technology, Springer-Verlag, Berlin, 1984, pp. 95–104.
[8] N. Laosiripojana, S. Charojrochkul, P. Kim-Lohsoontorn, S. Assabumrungrat, J. Catal. 276 (2010) 6–15.
[9] A.L. Vincent, J.-L. Luo, K.T. Chuang, A.R. Sanger, Appl. Catal. B 106 (2011) 114–122.
[10] A. Erdöhelyi, K. Fodor, T. Szailer, Appl. Catal. B 53 (2004) 153–160.
[11] M. Ziolek, J. Kujava, O. Saur, J.C. Lavalley, J. Mol. Catal. A 97 (1995) 49–55.
[12] J.R. Sohn, H.W. Kim, J. Mol. Catal. 52 (1989) 361–374.
[13] C.R. Vera, C.L. Pieck, K. Shimizu, J.M. Parera, Appl. Catal. A 230 (2002) 137–151.
[14] G.D. Yadav, J.J. Nair, Microporous Mesoporous Mater. 33 (1999) 1–48.
[15] J.R. Anderson, H. Kleinke, H.F. Franzen, J. Alloys Compd. 259 (1997) L14–L18.
[16] A. Travert, O.V. Manoilova, A.A. Tsyganenko, F. Maugé, J.C. Lavalley, J. Phys. Chem. B 106 (2002) 1350–1362.
[17] E.I. Kauppi, E.H. Rönkkönen, S.M.K. Airaksinen, S.B. Rasmussen, M.A. Bañares, A.O.I. Krause, Appl. Catal. B. 111–112 (2012) 605–613.
[18] A. Datta, R.G. Cavell, J. Phys. Chem. 89 (1985) 450–454.
[19] T. Viinikainen, H. Rönkkönen, H. Bradshaw, H. Stephenson, S. Airaksinen, M. Reinikainen, P. Simell, O. Krause, Appl. Catal. A 362 (2009) 169.
[20] T. Viinikainen, I. Kauppi, S. Korhonen, L. Lefferts, J. Kanervo, J. Lehtonen, Appl. Catal. B 142–143 (2013) 769–779.
[21] T. Song, M. Zhang, 4th International Conference on Bioinformatics and Biomedical Engineering (iCBBE), Chengdu, China, 18–20 June, 2010, pp. 1–4.
[22] V. Bolis, C. Morterra, M. Volante, L. Orio, B. Fubini, Langmuir 6 (1990) 695–701.
[23] D. Bianchi, T. Chafik, M. Khalfallah, S.J. Teichner, Appl. Catal. A 123 (1995) 89–110.
[24] C. Morterra, L. Orio, Mater. Chem. Phys. 24 (1990) 247–268.
[25] D.D. Beck, J.M. White, C.T. Ratcliffe, J. Phys. Chem. 90 (1986) 3123–3131.
[26] T. Zhu, L. Kundakovic, A. Dreher, M. Flytzani-Stephanopoulos, Catal. Today 50 (1999) 381–397.
[27] C.L. Liu, T.T. Chuang, I.G. Dalla Lana, J. Catal. 26 (1972) 474–476.
[28] A.M. Deane, D.L. Griffiths, I.A. Lewis, J.A. Winter, A.J. Tench, J. Chem. Soc. Faraday Trans. 1 (75) (1975) 1005.
[29] T.J. Toops, M. Crocker, Appl. Catal. B 82 (2008) 199–207.
[30] A. Clearfield, J. Am. Chem. Soc. 80 (1958) 6511–6513.
[31] W. Hertl, Langmuir 5 (1989) 96–100.
[32] J. Kondo, H. Abe, Y. Sakata, K. Maruya, K. Domen, T. Onishi, J. Chem. Soc. Faraday Trans. 1 (842) (1988) 511–519.

[33] P.O. Graf, D.J.M. de Vlieger, B.L. Mojet, L. Lefferts, J. Catal. 262 (2009) 181–187.
[34] D.G. Rethwisch, J.A. Dumesic, Langmuir 2 (1986) 73–79.
[35] X. Mugniery, T. Chafik, M. Primet, D. Bianchi, Catal. Today 52 (1999) 15–22.
[36] S. Kouva, J. Andersin, K. Honkala, J. Lehtonen, L. Lefferts, J. Kanervo, Phys. Chem. Chem. Phys. 16 (38) (2014) 20650–20664.
[37] B. Bachiller-Baeza, I. Rodriguez-Ramos, A. Guerrero-Ruiz, Langmuir 14 (1998) 3556–3564.
[38] P. Stelmachowski, S. Sirotin, P. Bazin, F. Maugé, A. Travert, Phys. Chem. Chem. Phys. 15 (2013) 9335–9342.
[39] A. Bampenrat, V. Meeyoo, B. Kitiyan, P. Rangsungvigit, T. Rirksomboon, Catal. Commun. 9 (2008) 2349–2352.